



Article

Investigation of Energy Transfer in Star-Shaped White Polymer Light-Emitting Devices via the Time-Resolved Photoluminescence

Hui He ^{1,2} , Xiaoqing Liao ², Jiang Cheng ², Ying Li ², Junsheng Yu ¹  and Lu Li ^{2,*}

¹ State Key Laboratory of Electronic Thin Films and Integrated Devices, School of Optoelectronic Science and Engineering, University of Electronic Science and Technology of China (UESTC), Chengdu 610054, China; hhe@std.uestc.edu.cn (H.H.); jsyu@uestc.edu.cn (J.Y.)

² Co-innovation Center for Micro/Nano Optoelectronic Materials and Devices, Research Institute for New Materials and Technology, Chongqing University of Arts and Science, Chongqing 402160, China; xiaoqin5122@163.com (X.L.); jiangcheng@cqwu.edu.cn (J.C.); leoyingchem@163.com (Y.L.)

* Correspondence: lli@cqwu.edu.cn; Tel.: +86-23-49512058

Received: 5 August 2018; Accepted: 8 September 2018; Published: 14 September 2018



Abstract: A series of white polymer light-emitting devices (WPLEDs) were fabricated by utilizing star-shaped white-emission copolymers containing tri[1-phenylisoquinolino-C2,N]iridium (Ir(piq)₃), fluorenone (FO) and poly(9,9-dioctylfluorene) (PFO) as red-, green- and blue-emitting (RGB) components, respectively. In these WPLEDs, a maximum current efficiency of 6.4 cd·A⁻¹ at 20 mA·cm⁻² and Commission Internationale d'Eclairage (CIE) coordinates of (0.33, 0.32) were achieved, and the current efficiency was still kept to 4.2 cd·A⁻¹ at the current density of 200 mA·cm⁻². To investigate energy transfer processes among the three different chromophores of the star-shaped copolymers in these WPLEDs, the time-resolved photoluminescence (PL) spectra were recorded. By comparing the fluorescence decay lifetimes of PFO chromophores in the four star-like white-emitting copolymers, the efficient energy transfer from PFO units to Ir(piq)₃ and FO chromophores was confirmed. From time-resolved PL and the analysis of energy transfer process, the results as follows were proved. Owing to the star-like molecular structure and steric hindrance effect, intermolecular interactions and concentrations quenching in the electroluminescence (EL) process could also be sufficiently suppressed. The efficient energy transfer also reduced intermolecular interactions' contribution to the enhanced device performances compared to the linear single-polymer white-light systems. Moreover, saturated stable white emission results from the joint of energy transfer and trap-assisted recombination. This improved performance is expected to provide the star-like white-emitting copolymers with promising applications for WPLEDs.

Keywords: star-shaped white polymer light-emitting devices; energy transfer; time-resolved photoluminescence; efficiency roll-off

1. Introduction

In the last few decades, white polymer light-emitting devices (WPLEDs) have gained remarkable attention because of their various applications in full-color displays with color filters, backlights, and solid-state lighting [1–8]. The low-cost solution processing offers WPLEDs great advantages over white organic light-emitting devices (WOLEDs) based on small molecules [9–11]. To fabricate WPLEDs with high performance, multilayer systems and blend systems have been widely employed; however, owing to the mixing of adjacent layers and phase separation, the device performances are not satisfactory. In contrast, the single-polymer white-emission systems can accomplish comparably stable bias-independent electroluminescence (EL) spectra, therefore, different kinds of single-polymer

white-emission systems including linear white-emitting polymer systems [12–14] and star-shaped white-light polymer systems [15,16] have already been developed. Compared with linear white-light polymers, due to effectively suppressed intermolecular interaction in the emitting layer (EML), the star-shaped white-light polymers exhibit higher EL efficiency for WPLEDs and have been more widely studied [17,18]. Wang et al. [19] recently reported a star-shaped white electroluminescent single-polymer system that employed two kinds of fluorescent dyes as orange cores and blue arms, respectively. A high current efficiency of $18 \text{ cd}\cdot\text{A}^{-1}$ was obtained in their single-layer devices utilizing the star-like white-emitting polymers as the active layer. Yang and his coworkers [20] also developed a series of new two-color star-shaped white-emission single polymers that simultaneously consist of fluorescent and phosphorescent dyes. However, as these star-shaped white-emitting polymers only comprise two complementary colors, the EL spectra of these polymers cannot cover the whole visible range and result in the limitation of applications.

In order to realize the saturated three-color white light, great efforts have been made by several groups to develop three-color star-shaped polymers with high-color-quality saturated white EL [21,22]. At the same time, in order to fabricate more efficient WPLEDs and further enhance EL performances of white-emitting polymers, many groups have also studied the mechanisms of white emission within the star-shaped white polymers [23–25]. But these previous investigations only involved two-color star-like copolymers or all-fluorescent star-like copolymers. Moreover, the energy transfer in three-color star-shaped white-emitting copolymers which comprise both fluorescent and phosphorescent chromophores has not yet been fully disclosed. Additionally, as an effective method that clarifies energy transfer in light-emitting devices, the time-resolved photoluminescence (PL) has been widely employed among blend light-emitting systems [26–28]; however, the investigation of energy transfer via the time-resolved photoluminescence on the star-like light-emitting copolymers is still scarce.

Therefore, the current work was carried out to investigate energy transfer between the host chromophores and guest chromophores in the three-color star-shaped white-light copolymers. In this work, a series of star-shaped copolymers reported previously [29], which comprise $\text{Ir}(\text{piq})_3$ core and poly(9,9-dioctylfluorene) (PFO) arms endcapped with a fluorenone (FO) unit, were utilized to fabricate the WPLEDs. The time-resolved PL of star-shaped copolymers both in dilute solution and in neat films were employed to demonstrate energy transfer processes in these three-color star-shaped copolymers. In addition, the energy transfer was classified by the PL spectra and EL spectra.

2. Materials and Methods

2.1. Materials

In our work, the star-like white copolymers were synthesized according to the reported synthesis procedure. The chemical structures of the monomers and the star-shaped copolymers are depicted in Figure 1. In the star-shaped copolymers, $\text{Ir}(\text{piq})_3$, FO and PFO (Energy Chemical, Shanghai, China) act as the red-, green- and blue-light-emitting units, respectively. The four kinds of monomers (M1, M2, M3 and M4) were synthesized into the star-shaped copolymers P1, P2, P3 and P4 at the different feed ratios of 1000:997.5:1:1, 1000:997.8:0.5:1, 1000:998.3:0.5:0.8 and 1000:998.75:0.5:0.5, respectively. Detailed synthesis procedures are described in [29].

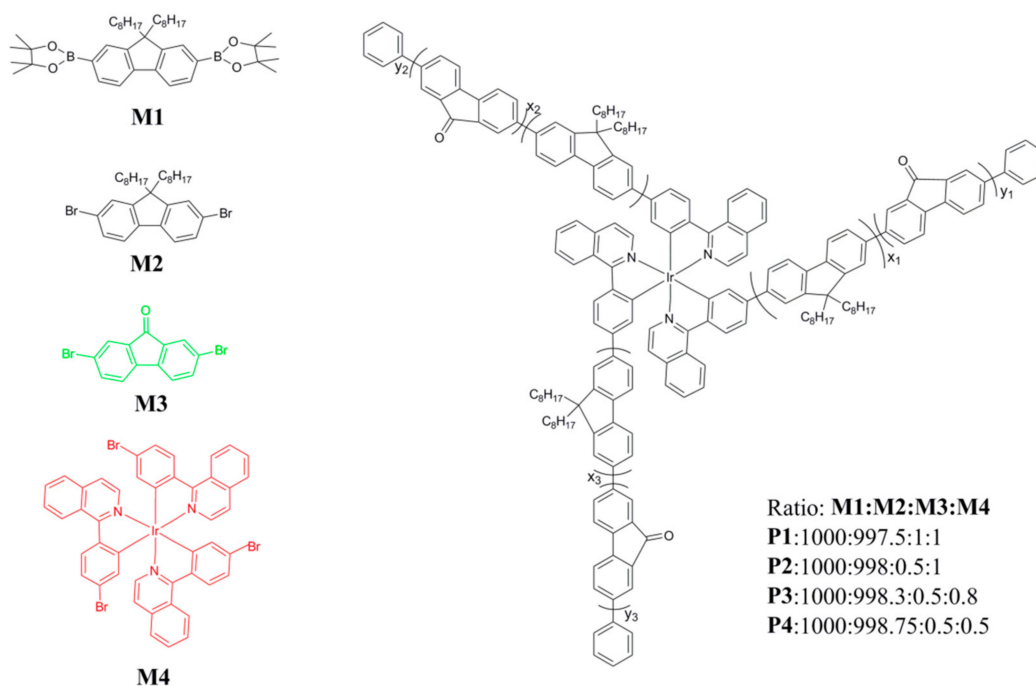


Figure 1. The chemical structures of the monomers and star-shaped white-emission copolymers.

2.2. The Fabrication of Devices and Measurements

WPLEDs were fabricated on the indium tin oxide (ITO)/glass substrates with a sheet resistance of $\sim 15 \Omega/\text{sq}$. First of all, the ITO/glass substrates were cleaned successively with detergent, deionized water, acetone and isopropanol for 15 min each step under ultrasonication, and then the substrates were treated with oxygen plasma to increase the work function and decrease the surface roughness. Poly(3,4-ethylenedioxythiophene):poly(styrenesulfonate) (PEDOT:PSS) (Heraeus, Shanghai, China) was spin-coated on the ITO/glass substrates at 3000 rpm for 60 s and then baked at 130°C . The resulting thin films were approximately 45 nm. The emitting materials in chlorobenzene ($10 \text{ mg}\cdot\text{mL}^{-1}$) (Sigma, Shanghai, China) were then spin-coated onto the PEDOT:PSS layer, and the solvent residue was removed after the emissive layer was annealed at 100°C for 30 min, and the resulting film was approximately 40 nm. Finally, a layer of 1,3,5-Tri(1-phenyl-1H-benzo[d]imidazole-2-yl)phenyl (TPBi (35 nm)) (Xi'an Polymer Light Technology Corp, Xi'an, China), a thin layer of LiF (1 nm) and a layer of aluminum (100 nm) were successively deposited in a vacuum thermal evaporator through a shadow mask at a base pressure of $5 \times 10^{-4} \text{ Pa}$. The resulting WPLEDs (devices A1, A2, A3, and A4, utilizing the polymers P1, P2, P3 and P4 as emitters, respectively) had a sandwiched configuration. Device structure and energy levels of the materials are shown as Figure 2. The active area of the devices was 0.12 cm^2 . Luminance–current density–voltage (L–J–V) characteristics were measured with a Keithley 2400 source (Keithley, Shanghai, China) and a calibrated silicon photodetector (Keithley, Shanghai, China). The EL spectra, Commission Internationale d’Eclairage (CIE) coordinate and the color rendering index (CRI) were recorded using a photoresearch PR-670 (Photo Research, Shanghai, China). The device fabrication and testing were carried out in a nitrogen-filled dry box with oxygen and moisture levels both below 0.1 ppm.

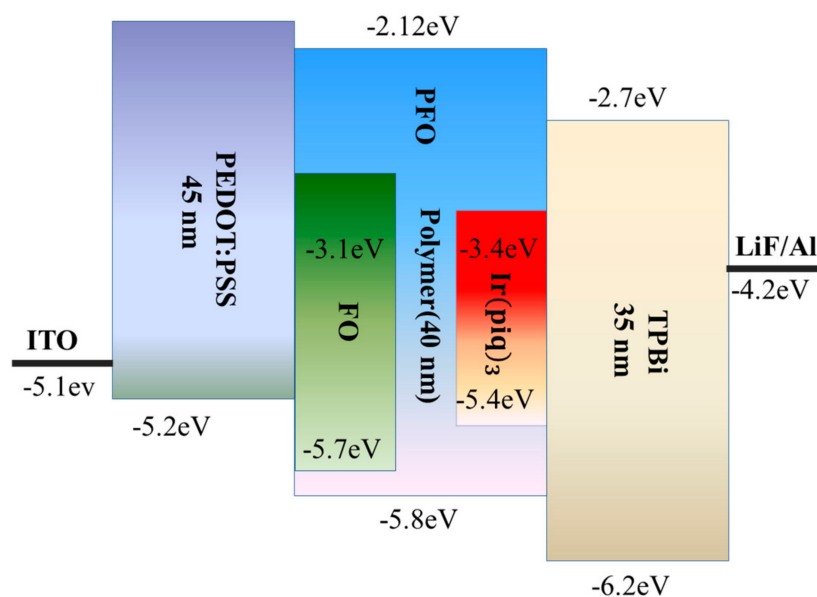


Figure 2. Device structure and energy levels of the materials.

3. Results and Discussions

3.1. Electrical Characteristics of the Devices

Figure 3a shows the L–J–V characteristics of the devices (see the double-logarithmic JV curves in Figure S1). It could be learned from the L–V curves that all devices show relatively high turn-on voltages (voltage at a luminance of 1 cd/m^2), ranging from 6.2 V to 6.5 V, and the luminance of the devices decreases with reducing content of FO and $\text{Ir}(\text{piq})_3$, and the maximum luminance of the A1, A2, A3 and A4 devices can reach $10,960 \text{ cd}\cdot\text{m}^{-2}$, $8421 \text{ cd}\cdot\text{m}^{-2}$, $5433 \text{ cd}\cdot\text{m}^{-2}$ and $3627 \text{ cd}\cdot\text{m}^{-2}$, respectively. Meanwhile, the J–V curves demonstrate a similar tendency with luminance of the devices from device A1 to device A4. Reasonable explanations for the current density and luminance behaviors of the devices can be given as follows. It can be seen from Figure 2 that the lowest unoccupied molecular orbital (LUMO) and highest occupied molecular orbital (HOMO) energy levels of FO (estimated to be -3.1 eV and -5.1 eV , respectively) and $\text{Ir}(\text{piq})_3$ (estimated to be -3.4 eV and -5.4 eV , respectively) lie between the LUMO (-2.12 eV) and HOMO (-5.8 eV) energy levels of PFO. When electrons and holes are injected into EML from the layers of PEDOT:PSS and TPBi, respectively, the sites of FO and $\text{Ir}(\text{piq})_3$ will act as traps for both electrons and holes in EML [26,30,31] and these carriers are trapped by these traps near the interface of EML, hindering the migration of these carriers towards the recombination region [32,33]. Therefore, more carriers need to be injected into the EML for white emission, which causes a larger current density. With increasing content of the red and green units (from device A4 to device A1), more triplet energy is utilized to produce light emission in the recombination region and lead to the higher device luminance. Figure 3b,c plot the current efficiency–current density (LE–J) characteristics and power efficiency–current density (PE–J) characteristics of WPLEDs, respectively. It can be observed that, with the content of $\text{Ir}(\text{piq})_3$ and FO increasing, the device efficiencies gradually enhance. The maximum current efficiencies and power efficiencies for the device A1–A4 are $5.9 \text{ cd}\cdot\text{A}^{-1}$ and $2.1 \text{ lm}\cdot\text{W}^{-1}$, $6.4 \text{ cd}\cdot\text{A}^{-1}$ and $2.3 \text{ lm}\cdot\text{W}^{-1}$, $5.2 \text{ cd}\cdot\text{A}^{-1}$ and $2 \text{ lm}\cdot\text{W}^{-1}$, $5.3 \text{ cd}\cdot\text{A}^{-1}$ and $1.8 \text{ lm}\cdot\text{W}^{-1}$, respectively. Figure 3b shows that the current efficiencies of device A1 and A2 still maintain high values at a current density $200 \text{ mA}\cdot\text{cm}^{-2}$, and the low efficiency roll-off is quite suitable for applications in flexible displays. The performances of WPLEDs are summarized in Table 1, and we can see that the device A2 exhibits the best performances with a high rendering index (CRI) of 91, and the 1931 CIE coordinates are (0.33, 0.32) (Figure S2), which are very close to standard white emission, (0.33, 0.33).

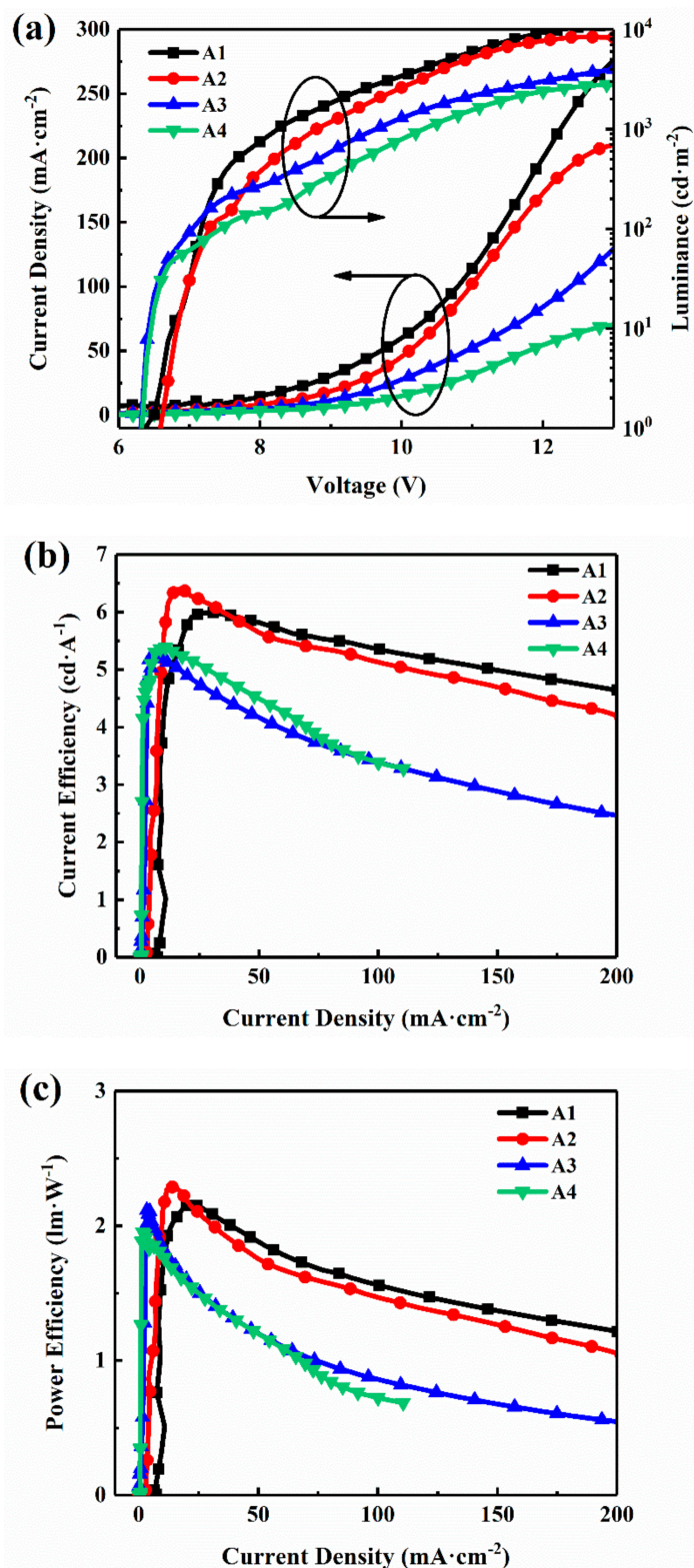


Figure 3. The performances of devices. (a) The current density–luminance–voltage (J–L–V) characteristics, (b) the current efficiency–current density (CE–J) characteristics, (c) the power efficiency–current density (PE–J) characteristics.

Figure 4a shows the normalized EL spectra of WPLEDs and the blue emission peaks (432 nm and 460 nm), green emission peak (540 nm) and red emission peak (628 nm) originating from PFO, FO and $\text{Ir}(\text{piq})_3$ chromophores, respectively. It can be seen that with the increase of the dopant units

content from copolymers P4-P1, the relative intensity of red emission and green emission peaks gets stronger (from the device A4 to A1). Figure 4b shows the EL spectra of device A2 at different voltages (10–15 V); the spectral shapes show slight changes in the range of 10 to 13 V, and the stable saturated white light is suitable for panel display and lighting. However, the charges become saturated for traps as the voltages are increased further, and more carriers generate radiative recombination on FPO arms and produce strong blue emission.

Table 1. Performance for white polymer light-emitting devices (WPLEDs) with polymers P1, P2, P3 and P4 as white-light emitters, respectively.

Device	Composition (Green:Red)	Max CE ($\text{cd}\cdot\text{A}^{-1}$)	Max PE ($\text{lm}\cdot\text{W}^{-1}$)	CIE ^a	CRI ^a
A1	1:1	5.9	2.1	(0.34, 0.35)	83
A2	0.5:1	6.4	2.3	(0.33, 0.32)	91
A3	0.5:0.8	5.2	2	(0.27, 0.34)	86
A4	0.5:0.5	5.3	1.8	(0.27, 0.26)	65

^a Commission Internationale d’Eclairage (CIE) and rendering index (CRI) were measured at a driving voltage of 10 V.

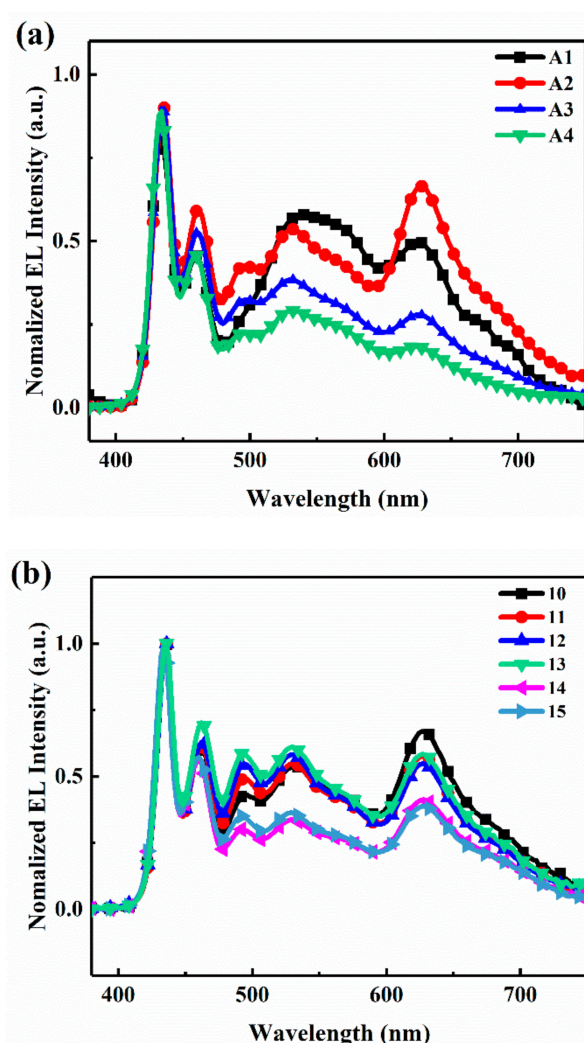


Figure 4. The spectral behaviors. (a) The normalized electroluminescence (EL) spectra of device A1–A4 at a driving voltage of 10 V, (b) the normalized EL spectra of device A2 at different voltages.

3.2. The Time-Resolved Photoluminescence and Energy Transfer within the White-Light Copolymers

In order to clarify the efficient energy transfer from PFO moieties to FO and Ir(piq)₃ units in EL process, the time-resolved fluorescence decays for PFO segments of the copolymers P1–P4 and the pure

PFO (linear PFO) both in solutions and in films were recorded as plotted in Figure 5a,b, respectively. The fluorescence decay can be well-fitted with a monoexponential decay curve. The fitting curve (Figure S3) can be described with Equation (1),

$$I_{PL}(t) = I_0 \exp[-(t/\tau^*)] + C \quad (1)$$

I_{PL} is the normalized photoluminescence intensity, and the constants I_0 and C represent the relative initial intensity of the emitted light at the end of the laser pulse and the relative background intensity due to the electrical driving and noise, respectively. The parameter τ^* represents the PL lifetime and is the main parameter in the fitting process [34]. The corresponding fluorescence lifetime values are listed in the Table 2.

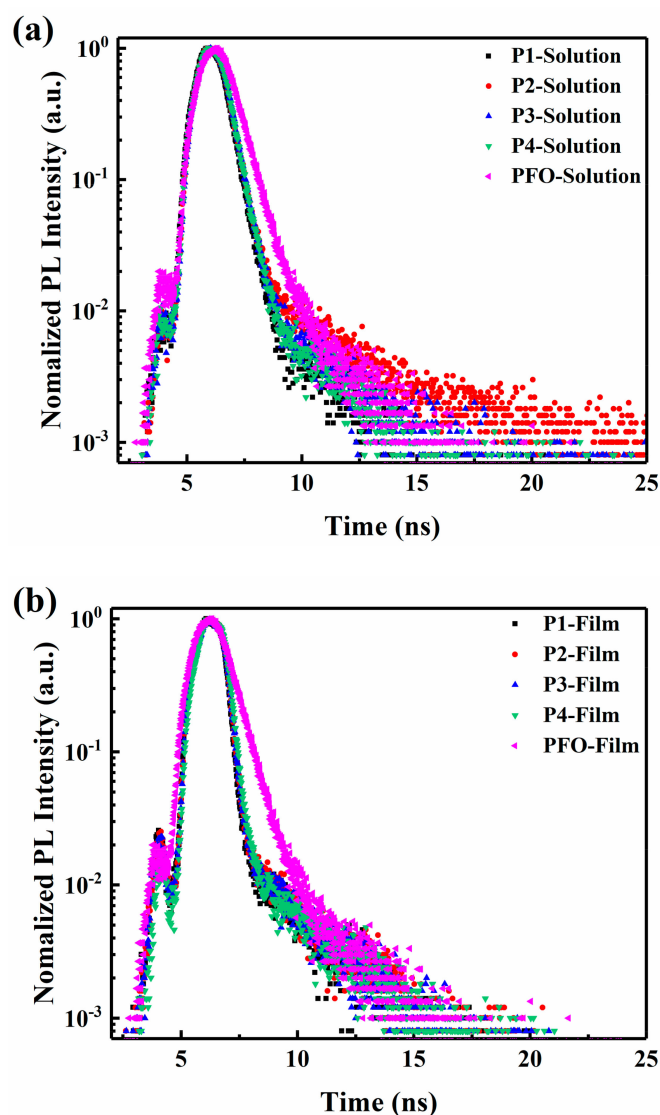


Figure 5. The time-resolved photoluminescence (PL) transients of P1–P4 and poly(9,9-dioctylfluorene) (PFO), (a) in Tetrahydrofuran(THF) solution (5×10^{-6} M), (b) in neat films ($\lambda_{ex} = 375$ nm, $\lambda_{em} = 423$ nm).

Table 2. The quantum yields, PL decay lifetime and energy transfer efficiency of polymers.

Polymer	$\Phi_{\text{PL}} (\%)$		$\tau (\text{ps})$		$E_t (\%)$
	Solution	Film	Solution	Film	
PFO	85	40	676	380	–
P1	80	28	467	221	57.5
P2	83	47	471	230	55.7
P3	84	42	472	240	53.8
P4	88	39	470	263	49.4

As shown in Figure 5a, the fluorescence transient decays in copolymer solutions are shorter than that in pure PFO solution; this is because for excited energy of pure PFO there are only two decay channels: the radiative decay channel and non-radiative relaxation, but for the excited energy of PFO in copolymers, there is the third decay channel: energy transfer, hence the excited PFO of copolymers have a faster relaxation and a shorter lifetime than that of pure PFO. It can be also seen from Table 2 that the fitted fluorescence lifetimes of copolymer P1–P4 in solution are 467 ps, 471 ps, 472 ps and 470 ps, respectively, and there is no clear difference to these lifetimes for the white emitting polymers P1–P4, which demonstrates relatively weak intramolecular energy transfer. The fitted decay lifetimes of PFO segments for copolymer P1, P2, P3 and P4 neat films are 221 ps, 230 ps, 240 ps and 263 ps, respectively, and are shorter than that in solution, which verifies more efficient energy transfer from PFO chains to Ir(piq)₃ and FO chromophores in copolymer neat films. The detailed energy transfer processes among the white-light polymers solution and neat films can be explained as follows. First of all, in ultra-dilute white-light polymer solutions, the white-emitting polymers are regarded as independent and separate from each other, and the intermolecular distance is beyond the Förster resonant energy transfer (FRET) radius R_0 , so intermolecular energy transfer from PFO chains to Ir(piq)₃ and FO units of adjacent white-emitting polymers are negligible. But in the same copolymer, singlet excitons produced in the fluorenes which are close to Ir(piq)₃ and FO chromophores could migrate to these red- and green-emission chromophores through intramolecular FRET processes. With the increase of conjugation and aggregation of copolymers in neat films, the distance of donor-accepter separation would typically be smaller than the Förster radius R_0 ; hence, intermolecular energy transfer from PFO segments to Ir(piq)₃ and FO segments are enhanced greatly. The combination of intramolecular and intermolecular transfer processes leads to a smaller fluorescence lifetime τ for the copolymer neat films. The fluorescence transient decays of the white-emission polymers both in solutions and in films present a long trail, and this phenomenon can be attributed to the existence of exciplexes, which lead to delayed emission.

On the other hand, the fluorescence lifetime corresponding to the blue emission of star-like PFO is around 520 ps [25], which is longer than that of linear PFO (380 ps) in the current work, indicating that the star-shaped structure can sufficiently suppress intermolecular interaction and reduce non-radiative relaxation. Additionally, the fluorescence decays get slower from P1 to P4, which demonstrates that energy transfer gradually becomes weakened, which is in accordance with the lower content of Ir(piq)₃ and FO chromophores leading to larger donor–accepter separation.

The different energy transfer mechanisms are also certified via the ultraviolet–visible (UV–vis) absorption spectra and the PL spectra of the monomers and the white-light copolymers. As shown in Figure 6a, there is an overlapped band between the UV–vis absorption spectrum of Ir(piq)₃ and the PL spectrum of PFO, indicating FRET from PFO segments to Ir(piq)₃ phosphor. Compared with Ir(piq)₃, there is a larger overlapped band between the UV–vis absorption spectrum of FO and the PL spectrum of PFO, indicating more efficient FRET from PFO segments to FO. The UV–vis absorption spectra and the PL spectra of the light-emitting copolymers P1–P4 in solutions and in films are displayed in Figure 6b,c, respectively. All copolymers both in solutions and in films present a very similar UV–vis absorption band with a peak wavelength at about 380 nm, which is assigned to the π – π^* transition of PFO backbone. It can be also seen in Figure 6b that the main emission peaks in solution are located at

about 420 nm and 440 nm, and the emission peak at 440 nm comes from the exciplex emission, which is consistent with a long trail of the fluorescence transient decays. Moreover, because the intramolecular energy transfer is so weak that no red and green emission are visible [13]. However, the PL spectra in films showed in Figure 6c exhibits the main blue emission peaks as well as the weak green emission originating from FO moieties, which is because simultaneous intramolecular and intermolecular FRET processes generate more excited FO units and result in stronger green emission peaks. The energy transfer efficiency (E_t) could be calculated from Equation (2) [35,36], where τ_0 is the lifetime of star-like PFO and τ' is the lifetime of copolymer films. The E_t is also listed in Table 2.

$$E_t = 1 - \frac{\tau'}{\tau_0} \quad (2)$$

It can be found that the values of transfer efficiency are gradually reduced from copolymer P1 to copolymer P4 with decreasing dopant unit content.

Additionally, due to more trap-assisted radiative recombination and more triplet emission in EL processes, the EL spectra show stronger green emission peaks and red emission peaks than those of PL spectra [37]. Figure 7 indicates the energy transfer processes among the different chromophores of the white-emission polymers in the EL process. The combination of efficient energy transfer and trap-assisted recombination generates saturated white emission, as is referred to from CE-J characteristics above, and the reduced intermolecular interaction resulting from the special spatial structure and energy transfer from PFO moieties to FO and Ir(piq)₃ units contribute to low efficiency roll-off [38,39].

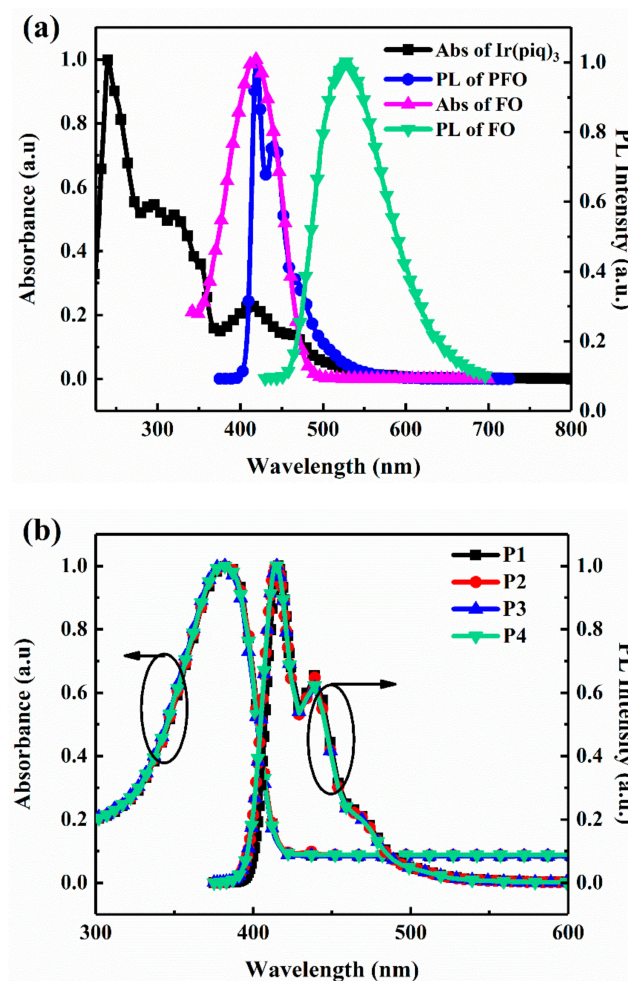


Figure 6. Cont.

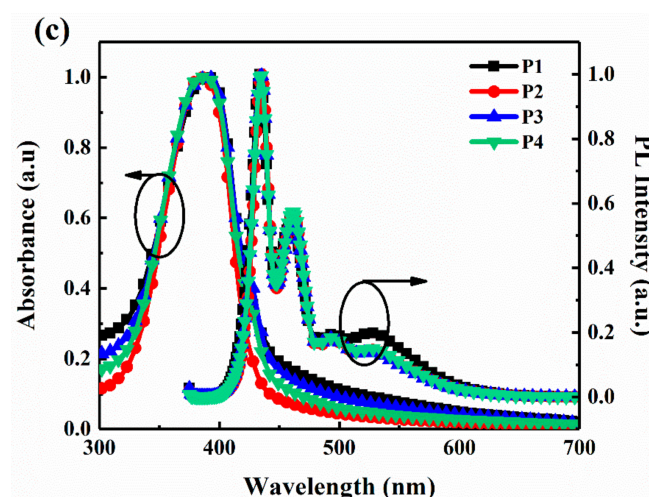


Figure 6. The ultraviolet–visible (UV–vis) absorption spectra and the normalized PL spectra, (a) the UV–vis absorption spectra of Ir(piq)₃ and fluorenone (FO) and the PL spectra of PFO and FO in THF solutions (5×10^{-6} M), and (b) the UV–vis absorption spectra and the normalized PL spectra of copolymers P1–P4 in THF solutions (5×10^{-6} M), (c) the UV–vis absorption spectra and the normalized PL spectra of copolymers P1–P4 in neat films ($\lambda_{\text{ex}} = 375$ nm, $\lambda_{\text{em}} = 423$ nm).

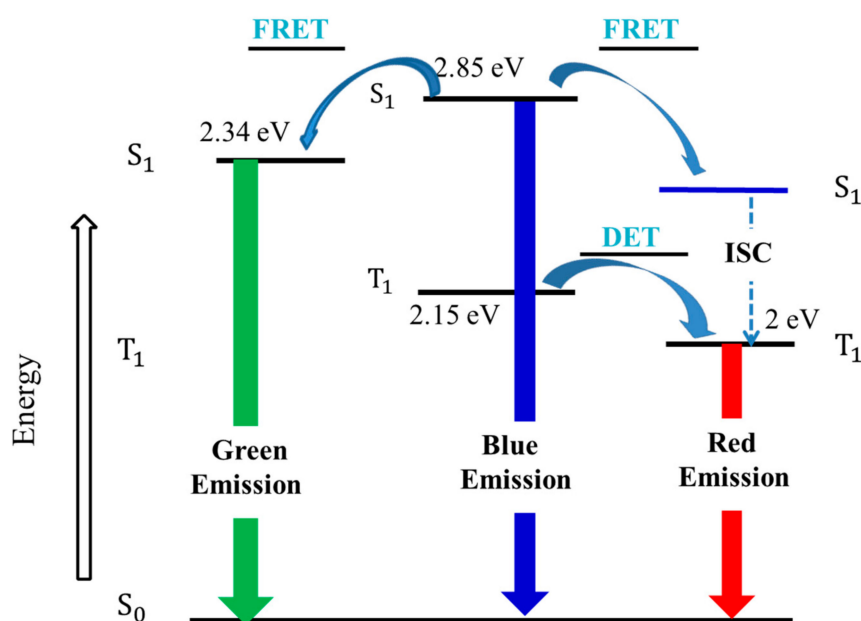


Figure 7. Exciton energy diagram of PFO, FO and Ir(piq)₃ and energy transfer processes.

4. Conclusions

In conclusion, a series of star-shaped WPLEDs were fabricated. Compared to the star-shaped WPLEDs reported previously, low-efficiency roll-off and saturated white emission in our systems were obtained. The comparison between the time-resolved fluorescent spectra shows that the excitation energy of PFO chains can efficiently transfer onto the FO and Ir(piq)₃ units in neat films by the FRET process containing intramolecular and intermolecular processes, and the star-shaped molecular structure can efficiently reduce intermolecular interaction. Through the analyses of PL spectra and EL spectra, we found that the white emission is due to the double effects of energy transfer and trap-assisted recombination in EL processes. Based on these conclusions, the EL performances of the promising star-shaped white-emitting copolymers containing both fluorescent and phosphorescent chromophores can be further enhanced by optimizing the device structure of WPLEDs.

Supplementary Materials: The following are available online at <http://www.mdpi.com/1996-1944/11/9/1719/s1>, Figure S1: The double-logarithmic JV curves, Figure S2: The 1931 CIE chromaticity diagram of emission of the WPLEDs; (a) the CIE coordinates of devices A1–A4 at a voltage of 10 V; (b) the CIE chromaticity diagram of device A2 at different voltages, Figure S3: The fit curves of the time-resolved PL for copolymers P1–P4; (a) the white-light copolymer in solutions; (b) the white-light copolymer in films.

Author Contributions: H.H., X.L., J.C. and Y.L. designed and carried out the experiments. H.H. and J.Y. analyzed the results and wrote the first draft of the manuscript. L.L. revised the manuscript and corrected the English. All authors read and approved the final manuscript.

Funding: This research was funded by the National Key Research and Development Program of China grant number 2018YFB0407100-02, the Foundations of National Natural Science Foundation of China (NSFC) (No. 51503022 and No. 61605138); the International Science and Technology Cooperation Program of China (2014DFR50830); the Foundation for Innovation Research Groups of the NSFC (No. 61421002); the Chongqing Science and Technology Commission (No. cstc2015jcyjA50036, No. cstc2016jcyjys50001 and No. cstc2016jcyj0367); the Qualified Personnel Foundation of Taiyuan University of technology (QPFT) (No. tyutrc201255a); the technology Project from Chongqing Education Committee (No. KJ160112 and No. KJ1401122); the Natural Science Foundation of Yongchuan District (No. Ycstc2015nc4001); the research project for Chongqing University of Arts and Sciences (No. z2016xc16); the Open Foundation of State Key Laboratory of Electronic Thin Films and Integrated Devices (No. kfj201507); the Scientific and Technological Research Program of Chongqing Municipal Education Commission (KJ1601114); the Talent Introduction Project of Chongqing University of Arts and Sciences (R2016XC14).

Conflicts of Interest: The authors declare no conflict of interests.

References

1. Liu, B.; Luo, D.; Zou, J.; Gao, D.; Ning, H.; Wang, L.; Peng, J.; Cao, Y. A host–guest system comprising high guest concentration to achieve simplified and high-performance hybrid white organic light-emitting diodes. *J. Mater. Chem. C* **2015**, *3*, 6359–6366. [[CrossRef](#)]
2. Hu, S.; Zhu, M.; Zou, Q.; Wu, H.; Yang, C.; Wong, W.; Yang, W.; Peng, J.; Cao, Y. Efficient hybrid white polymer light-emitting devices with electroluminescence covered the entire visible range and reduced efficiency roll-off. *Appl. Phys. Lett.* **2012**, *100*, 63304. [[CrossRef](#)]
3. Zou, J.; Liu, J.; Wu, H.; Yang, W.; Peng, J.; Cao, Y. High-efficiency and good color quality white light-emitting devices based on polymer blend. *Org. Electron.* **2009**, *10*, 843–848. [[CrossRef](#)]
4. Vollbrecht, J.; Wiebeler, C.; Neuba, A.; Bock, H.; Schumacher, S.; Kitzerow, H. Bay-Extended, distorted perylene esters showing visible luminescence after ultraviolet excitation: Photophysical and electrochemical analysis. *J. Phys. Chem. C* **2016**, *120*, 7839–7848. [[CrossRef](#)]
5. Shoustikov, A.; You, Y.; Thompson, M. Electroluminescence color tuning by dye doping in organic Light-Emitting diodes. *IEEE J. Sel. Top. Quant.* **1998**, *4*, 3–13. [[CrossRef](#)]
6. Vollbrecht, J.; Blazy, S.; Dierks, P.; Peurifoy, S.; Bock, H.; Kitzerow, H. Electroluminescent and optoelectronic properties of OLEDs with Bay-Extended, distorted perylene esters as emitter materials. *ChemPhysChem* **2017**, *18*, 2024–2032. [[CrossRef](#)] [[PubMed](#)]
7. Zhao, D.; Qin, Z.; Huang, J. Progress on material, structure and function for tandem organic light-emitting diodes. *Org. Electron.* **2017**, *51*, 220–242. [[CrossRef](#)]
8. Zhao, D.; Wu, M.; Qin, R.; Yu, J. Low dark-current and high-photodetectivity transparent organic ultraviolet photodetector by using polymer-modified ZnO as the electron transfer layer. *Opt. Lett.* **2018**, *43*, 3212–3215. [[CrossRef](#)] [[PubMed](#)]
9. Liu, J.; Guo, X.; Bu, L.; Xie, Z.; Cheng, Y.; Geng, Y.; Wang, L.; Jing, X.; Wang, F. White electroluminescence from a single-polymer system with simultaneous two-color emission: Polyfluorene blue host and side-chain-located orange dopant. *Adv. Funct. Mater.* **2007**, *17*, 1917–1925. [[CrossRef](#)]
10. Liu, J.; Shao, S.; Chen, L.; Xie, Z.; Cheng, Y.; Geng, Y.; Wang, L.; Jing, X.; Wang, F. White electroluminescence from a single polymer system: Improved performance by means of enhanced efficiency and red-shifted luminescence of the blue-light-emitting species. *Adv. Mater.* **2007**, *19*, 1859–1863. [[CrossRef](#)]
11. Luo, J.; Li, X.; Hou, Q.; Peng, J.; Yang, W.; Cao, Y. High-efficiency white-light emission from a single copolymer: Fluorescent blue, green, and red chromophores on a conjugated polymer backbone. *Adv. Mater.* **2007**, *19*, 1113–1117. [[CrossRef](#)]
12. Liu, J.; Li, L.; Pei, Q. Conjugated polymer as host for high efficiency blue and white electrophosphorescence. *Macromolecules* **2011**, *44*, 2451–2456. [[CrossRef](#)]

13. Wang, H.; Xu, Y.; Tsuboi, T.; Xu, H.; Wu, Y.; Zhang, Z.; Miao, Y.; Hao, Y.; Liu, X.; Xu, B.; Huang, W. Energy transfer in polyfluorene copolymer used for white-light organic light emitting device. *Org. Electron.* **2013**, *14*, 827–838. [[CrossRef](#)]
14. Vollbrecht, J. Excimers in organic electronics. *New J. Chem.* **2018**, *42*, 11249–11254. [[CrossRef](#)]
15. Jiu, Y.; Liu, C.; Wang, J.; Lai, W.; Jiang, Y.; Xu, W.; Zhang, X.; Huang, W. Saturated and stabilized white electroluminescence with simultaneous three-color emission from a six-armed star-shaped single-polymer system. *Polym. Chem.* **2015**, *6*, 8019–8028. [[CrossRef](#)]
16. Zhao, Y.; Lin, Z.; Zhou, Z.; Yao, H.; Lv, W.; Zhen, H.; Ling, Q. White light-emitting devices based on star-shape like polymers with diarylmaleimide fluorophores on the side chain of polyfluorene arms. *Org. Electron.* **2016**, *31*, 183–190. [[CrossRef](#)]
17. Wang, J.; Zhang, F.; Liu, B.; Xu, Z.; Zhang, J.; Wang, Y. Emission colour-tunable phosphorescent organic light-emitting diodes based on the self-absorption effect and excimer emission. *J. Phys. D Appl. Phys.* **2013**, *46*, 15104. [[CrossRef](#)]
18. Sun, J.; Yang, J.; Zhang, C.; Wang, H.; Li, J.; Su, S.; Xu, H.; Zhang, T.; Wu, Y.; Wong, W.; Xu, B. A novel white-light-emitting conjugated polymer derived from polyfluorene with a hyperbranched structure. *New J. Chem.* **2015**, *39*, 518–5188. [[CrossRef](#)]
19. Chen, L.; Li, P.; Cheng, Y.; Xie, Z.; Wang, L.; Jing, X.; Wang, F. White electroluminescence from star-like single polymer systems: 2,1,3-Benzothiadiazole derivatives dopant as orange cores and polyfluorene host as six blue arms. *Adv. Mater.* **2011**, *23*, 2986–2990. [[CrossRef](#)] [[PubMed](#)]
20. Zhu, M.; Li, Y.; Cao, X.; Jiang, B.; Wu, H.; Qin, J.; Cao, Y.; Yang, C. White polymer light-emitting diodes based on star-shaped polymers with an orange dendritic phosphorescent core. *Macromol. Rapid Comm.* **2014**, *35*, 2071–2076. [[CrossRef](#)] [[PubMed](#)]
21. Sun, J.; Wang, H.; Xu, H.; Zhang, T.; Li, L.; Li, J.; Wu, Y.; Xu, B.; Zhang, X.; Lai, W. A novel high-efficiency white hyperbranched polymer derived from polyfluorene with green and red iridium(III) complexes as the cores. *Dyes Pigm.* **2016**, *130*, 191–201. [[CrossRef](#)]
22. Jiu, Y.; Wang, J.; Yi, J.; Liu, C.; Zhang, X.; Lai, W.; Huang, W. High-color-quality white electroluminescence and amplified spontaneous emission from a star-shaped single-polymer system with simultaneous three-color emission. *Polym. Chem.* **2017**, *8*, 851–859. [[CrossRef](#)]
23. Yan, Q.; Yue, K.; Yu, C.; Zhao, D. Oligo- and polyfluorene-tethered fac-Ir(ppy)₃: Substitution effects. *Macromolecules* **2010**, *43*, 8479–8487. [[CrossRef](#)]
24. Liu, C.; Jiu, Y.; Wang, J.; Yi, J.; Zhang, X.; Lai, W.; Huang, W. Star-shaped single-polymer systems with simultaneous RGB emission: Design, synthesis, saturated white electroluminescence, and amplified spontaneous emission. *Macromolecules* **2016**, *49*, 2549–2558. [[CrossRef](#)]
25. Zhao, Y.; Yao, H.; Wei, K.; Zhen, H.; Yang, E.; Lin, Z.; Ling, Q. Dual-core star-shaped single white polymers: The effect of host structure on luminescence properties. *Phys. Chem. Chem. Phys.* **2017**, *19*, 12642–12646. [[CrossRef](#)] [[PubMed](#)]
26. Su, S.; Cai, C.; Takamatsu, J.; Kido, J. A host material with a small singlet–triplet exchange energy for phosphorescent organic light-emitting diodes: Guest, host, and exciplex emission. *Org. Electron.* **2012**, *13*, 1937–1947. [[CrossRef](#)]
27. Reineke, S.; Lindner, F.; Schwartz, G.; Seidler, N.; Walzer, K.; Lüssem, B.; Leo, K. White organic light-emitting diodes with fluorescent tube efficiency. *Nature* **2009**, *459*, 234–238. [[CrossRef](#)] [[PubMed](#)]
28. Shaw, P.E.; Ruseckas, A.; Samuel, I.D.W. Distance dependence of excitation energy transfer between spacer-separated conjugated polymer films. *Phys. Rev. B* **2008**, *78*, 245201. [[CrossRef](#)]
29. Zhang, T.; Sun, J.; Liao, X.; Hou, M.; Chen, W.; Li, J.; Wang, H.; Li, L. Poly(9,9-dioctylfluorene) based hyperbranched copolymers with three balanced emission colors for solution-processable hybrid white polymer light-emitting devices. *Dyes Pigm.* **2017**, *139*, 611–618. [[CrossRef](#)]
30. Zuo, G.; Li, Z.; Andersson, O.; Abdalla, H.; Wang, E.; Kemerink, M. Molecular doping and trap filling in organic semiconductor host–guest systems. *J. Phys. Chem. C* **2017**, *121*, 7767–7775. [[CrossRef](#)]
31. Zhang, K.; Chen, Z.; Yang, C.; Tao, Y.; Zou, Y.; Qin, J.; Cao, Y. Stable white electroluminescence from single fluorene-based copolymers: Using fluorenone as the green fluorophore and an iridium complex as the red phosphor on the main chain. *J. Mater. Chem.* **2008**, *18*, 291–298. [[CrossRef](#)]
32. Mandoc, M.M.; de Boer, B.; Paasch, G.; Blom, P.W.M. Trap-limited electron transport in disordered semiconducting polymers. *Phys. Rev. B* **2007**, *75*, 193202. [[CrossRef](#)]

33. Lee, J.; Lee, S.; Yoo, S.; Kim, K.; Kim, J. Langevin and trap-assisted recombination in phosphorescent organic light emitting diodes. *Adv. Funct. Mater.* **2014**, *24*, 4681–4688. [[CrossRef](#)]
34. Wehrmeister, S.; Ger, L.J.; Wehler, T.; Rausch, A.F.; Reusch, T.C.G.; Schmidt, T.D.; Brütting, W. Combined electrical and optical analysis of the efficiency roll-off in phosphorescent organic light-emitting diodes. *Phys. Rev. Appl.* **2015**, *3*, 24008. [[CrossRef](#)]
35. Huang, J.; Goh, T.; Li, X.; Sfeir, M.Y.; Bielinski, E.A.; Tomasulo, S.; Lee, M.L.; Hazari, N.; Taylor, A.D. Polymer bulk heterojunction solar cells employing Forster resonance energy transfer. *Nat. Photonics* **2013**, *7*, 480–486. [[CrossRef](#)]
36. Zhao, J.; Wang, Z.; Wang, R.; Chi, Z.; Yu, J. Hybrid white organic light-emitting devices consisting of a non-doped thermally activated delayed fluorescent emitter and an ultrathin phosphorescent emitter. *J. Lumin.* **2017**, *184*, 287–292. [[CrossRef](#)]
37. Wetzelaer, G.A.H.; Kuik, M.; Nicolai, H.T.; Blom, P.W.M. Trap-assisted and Langevin-type recombination in organic light-emitting diodes. *Phys. Rev. B* **2011**, *83*, 165204. [[CrossRef](#)]
38. Jiang, Z.; Ye, T.; Yang, C.; Yang, D.; Zhu, M.; Zhong, C.; Qin, J.; Ma, D. Star-shaped oligotriarylamines with planarized triphenylamine core: Solution-processable, high-Tg hole-injecting and hole-transporting materials for organic light-emitting devices. *Chem. Mater.* **2011**, *23*, 771–777. [[CrossRef](#)]
39. Chen, L.; Zhang, C.; Lin, G.; Nie, H.; Luo, W.; Zhuang, Z.; Ding, S.; Hu, R.; Su, S.; Huang, F.; et al. Solution-processable, star-shaped bipolar tetraphenylethene derivatives for the fabrication of efficient nondoped OLEDs. *J. Mater. Chem. C* **2016**, *4*, 2775–2783. [[CrossRef](#)]



© 2018 by the authors. Licensee MDPI, Basel, Switzerland. This article is an open access article distributed under the terms and conditions of the Creative Commons Attribution (CC BY) license (<http://creativecommons.org/licenses/by/4.0/>).